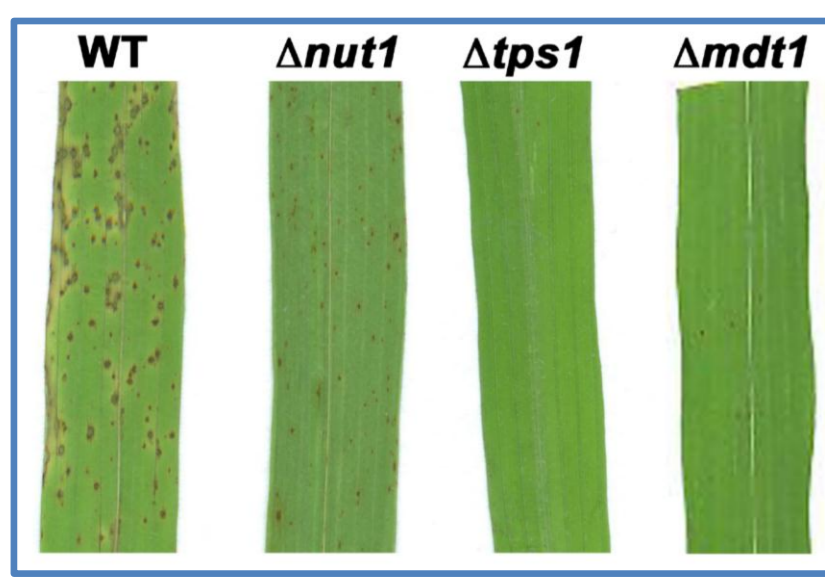


¹ Agilent Technologies, 5300 Stevens Creek Blvd, Santa Clara, CA, United States
² Department of Plant Pathology - University of Nebraska at Lincoln, 406 Plant Sciences Hall, Lincoln, NE, United States
³ GC Image LLC, 201 N 8th St # 420, Lincoln, NE, United States
⁴ Zoex Corporation, 12221 Fuqua St, Houston, TX, United States

Introduction



The rice blast fungus *Magnaporthe oryzae* is a widely spread plant pathogen that causes significant losses of rice and wheat production and is a global food security threat (Wilson and Talbot, *Nat Rev Microbiol* 7:185–195, 2009; Fernandez and Wilson, *Mol Plant Microbe Interact* 25: 1286–1293, 2012). Foliar infection requires a specialized cell called an appressorium that forms on the surface of the rice leaf and generates enormous hydrostatic turgor. This forces a thin penetration hypha through the rice cuticle and into the underlying epidermal cells, where it grows for the first days of infection as a symptomless biotroph before entering its destructive necrotrophic stage (Fernandez and Wilson, *Protoplasma* 251: 37–47, 2014). However, the metabolic strategies employed by *M. oryzae* to colonize rice cells are unknown. Understanding more about nutrient acquisition and utilization in *M. oryzae* would shed light on the infection process and might point to new avenues for effective disease management. In this study, we have compared the partial metabolomes of a wild type strain of *M. oryzae* (Guy11) to non-pathogenic mutant strains that result from the deletion of genes encoding a nitrogen regulator ($\Delta nut1$), a carbon regulator ($\Delta mdt1$) and an integrator of carbon and nitrogen metabolism ($\Delta tps1$) (Fernandez et al., *PLoS Genet* 8: e1002673, 2012) (Fig. 1). Information gained from these analyses will enhance our understanding of how *M. oryzae* controls metabolism, and how nutrient is assimilated during growth.

Fig 1. Rice foliar infection of wild type *M. oryzae* (Guy11 isolate) and the $\Delta nut1$, $\Delta tps1$ and $\Delta mdt1$ deletion mutants. The susceptible rice cultivar CO-39 was inoculated with 1×10^5 spores/ml of each strain. Leaves were imaged 5 days after inoculation.

Experimental

Samples

Mutants were grown under minimal media shake conditions in the presence of 1% (w/v) glucose and 10 mM nitrate as sole carbon and nitrogen sources, respectively. Mycelial tissue samples were collected, lyophilized, and ground in liquid nitrogen. The metabolites were extracted using a mixture of methanol:chloroform:water (1:2.5:1, v/v/v). Internal standard (d27-myristic acid) was added to each sample. The extracts were dried under vacuum and derivatized by methoximation followed by silylation with MSTFA + 1% TMCS. The samples were analyzed using GC x GC x QTOFMS (Fig. 2) methodology. GC x GC x QTOFMS parameters are described in Table 1.

Instrument and method parameters

Instrument	Agilent 7890B/ZOEX ZX2 thermal modulation system Agilent 7200 Q-TOF
Columns	(1) 15.0 m x 0.25 mm ID x 0.25 μ m HP-5MS Ultra Inert, (2) 3.25 m x 0.1 mm ID x 0.1 μ m SGE BPX-50
Carrier Gas	Helium
Column Flow	1.2 mL/min, constant flow
Auto-sampler	Agilent 7693A
Injection Port	Split/Splitless Inlet
Inlet Temperature	280 °C
Injection Volume	1.0 μ L
Split Ratio	15:1
Oven Program	60 °C (0 min) – 3 °C/min – 310 (0 min)
Modulation Period	6.8 sec
Cold Jet Flow	13 L/min
Hot Jet Temperature	375 °C
Hot Jet Duration	320 msec
Interface Temp	310 °C
Source Temp.	300 °C
Quad. Temp.	150 °C
Mass Range	m/z 60 – 650
Data Rate	50 Hz
Ionization Mode	EI, positive CI (20% methane flow)
Emission Current	35 μ A (EI), 240 μ A (CI)
Electron Energy	70 eV (EI), 80 eV (CI)

Table 1. GC x GC and QTOF conditions

Identification of the significant metabolomic differences between wild type strain and non-pathogenic mutants

In this study, we employed GC x GC methodology to compare partial metabolomes of a wild type (WT) isolate of *M. oryzae* to non-pathogenic mutant strains resulting from targeted deletion of key metabolic regulatory genes. The data were acquired in both EI and positive CI modes to enhance identification of unknown metabolites. The data were processed and visualized using both GC Image and GCxGC Hi-res Edition software (pre-release version 2.5a0) as well as MassHunter Qualitative Analysis (pre-released version B.07) software tools. As a first step, the data files were imported into GC Image for further processing. Each chromatogram was analyzed using a template comprising 1) peaks common to all chromatograms ("reliable peaks") for image alignment purposes, and 2) common peak-region features for quantitative image comparison. The reliable peaks were determined from the bidirectional pairwise matching of all possible pairs of chromatograms (Reichenbach et al., *Anal Chem*, 85:4974, 2013). The peak-region features were delineated by peak detection in the composite chromatogram created by registering and summing all chromatograms (Reichenbach et al., *J Chromatogr A*, 1226:140, 2012). The total intensity count (TIC) in each peak-region of each chromatogram in each sample class was used to compute the Fisher Discriminate Ratio (FDR) between classes for each feature.

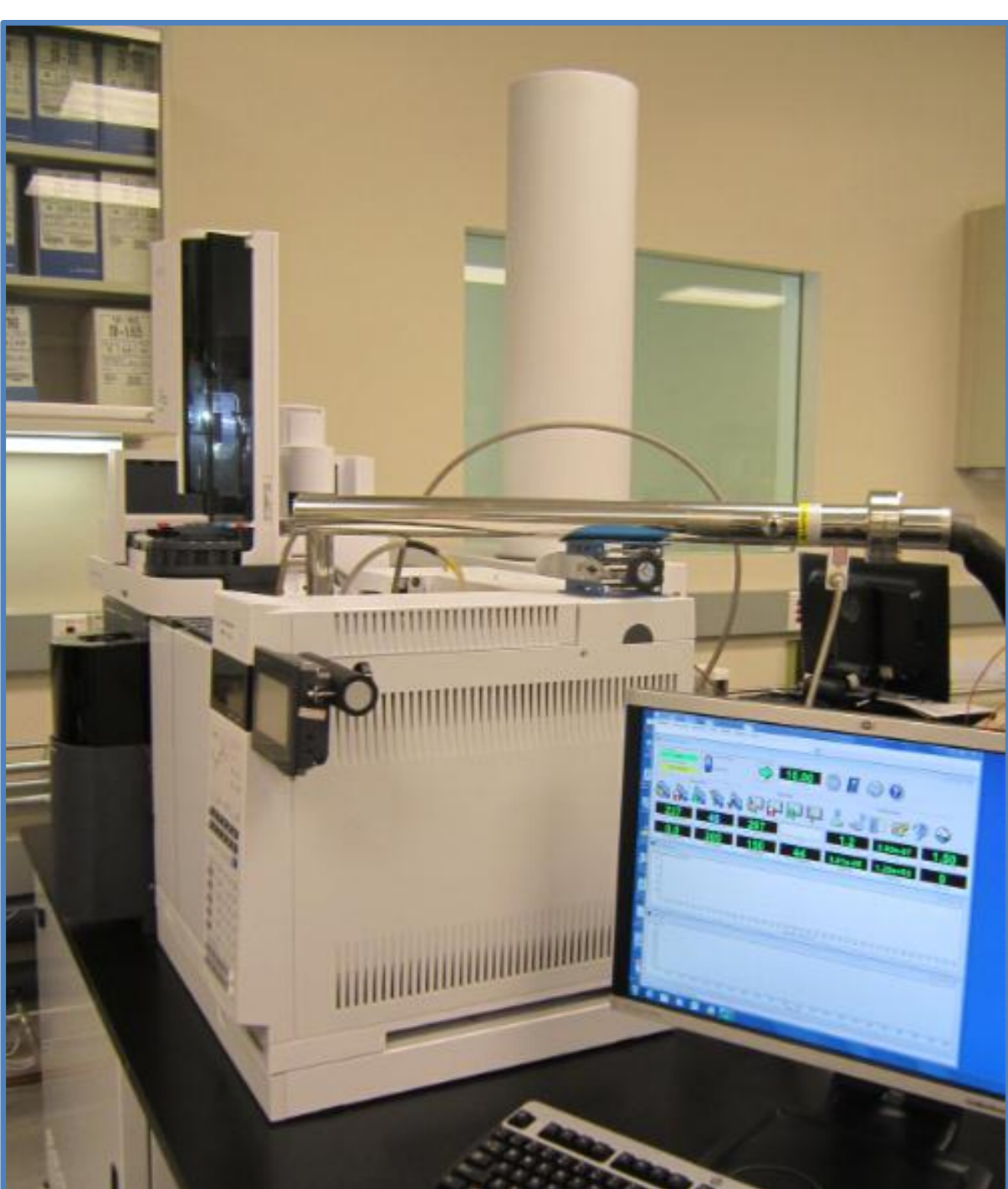


Fig 2. GC x GC x QTOF system

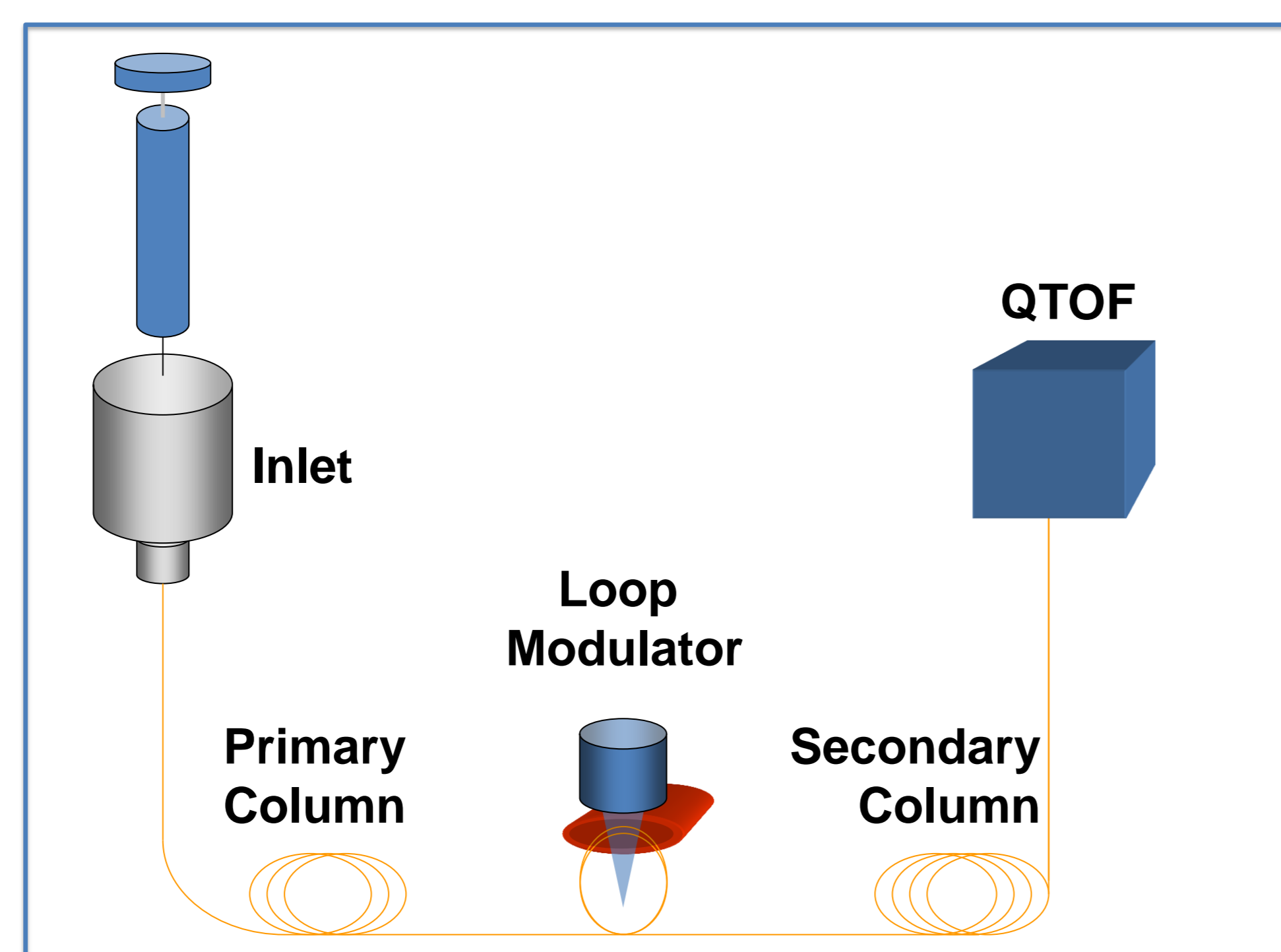


Fig3. GC x GC Layout

GC x GC configuration

The GC x GC system employed a loop thermal modulator (Model ZX-2, Zoex Corporation, Houston, TX). Analyte bands eluting from the primary column were cryogenically accumulated, focused, and remobilized every 6.8 seconds (modulation period), thereby injecting a series of "cuts" from the first column onto the second. High speed secondary chromatograms developed on the second column, completing elution within the 6.8 second modulation period. The QTOF MS acquired high mass resolution spectra of the secondary column effluent at a rate of 50 full scan spectra per second.

Results and Discussion

Metabolic Responses

Data files from the QTOF were transformed into GC Image (See Fig.4), which were further processed in order to identify compounds exhibiting large variation between wild type and mutant strains, as indicated by FDR values obtained from pairwise comparison of TIC intensities. The levels of numerous metabolites in the various mutant strains differed significantly. Many of the metabolites were identified (Fig.4). Key statistics, including the FDR for each metabolite identified, are reported in Table 2.

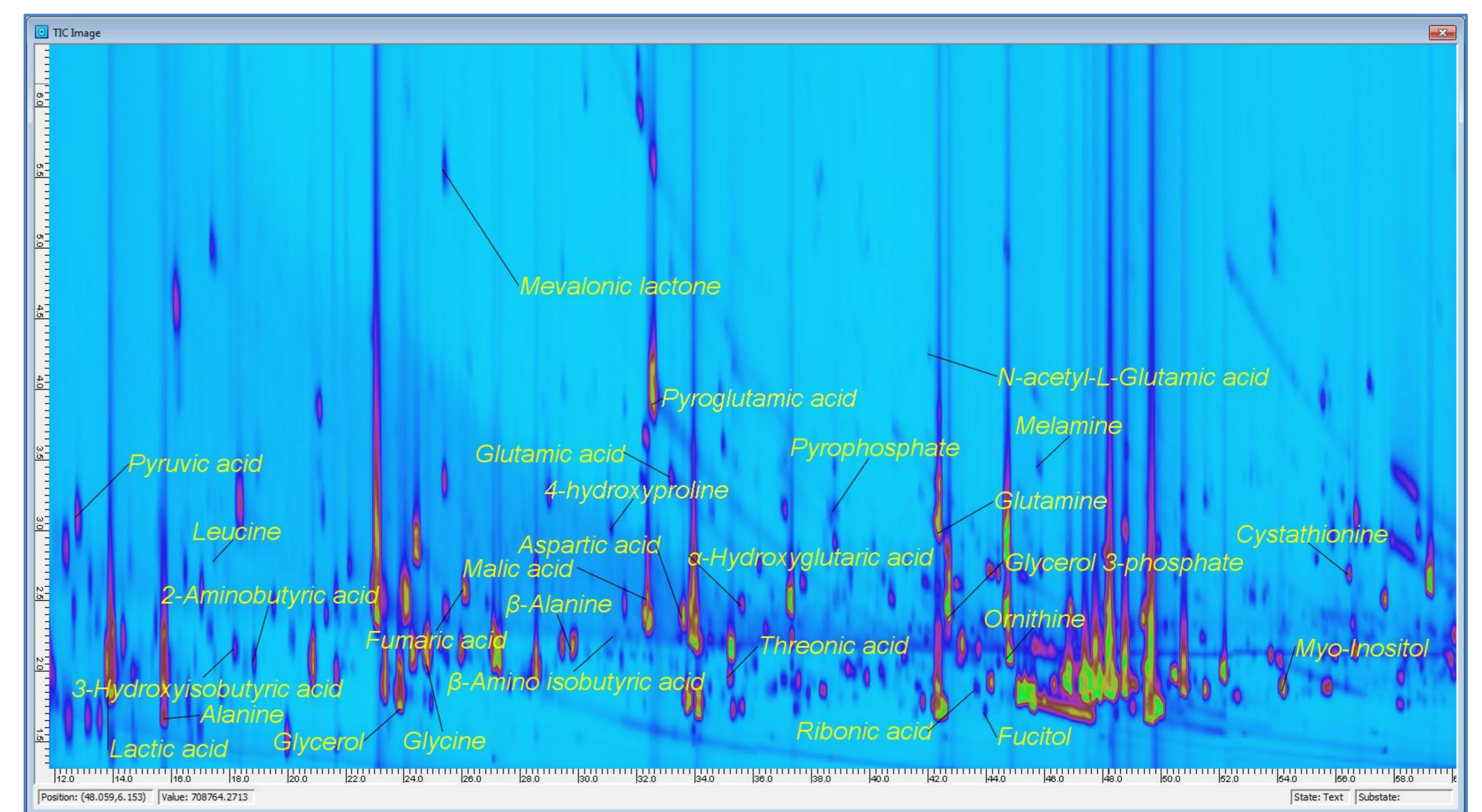


Fig 4. Labels indicate identified metabolites, the signal intensities of which differ significantly between wild type (Guy11) and at least one deletion mutant

RT1	RT2	Volume	%Response	FDR	Gny11,dMDT1	Gny11,dNut1	Gny11,dTPS1	dMDT1,dNut1	dMDT1,dTPS1	dNut1,dTPS1	Compound ID
56.42	2.64	22117834	0.0478	142.68	43.89	163.21	196.32	1.25	1.14	0.05	Cystathionine
42.27	2.95	45539643	0.0852	95.11	30.28	36.15	30.88	33.05	0.47	3.85	Glutamine
43.57	1.87	24377223	0.0480	63.38	68.99	1.83	66.34	24.61	0.24	23.84	Ribonic acid
45.39	1.81	126431935	0.2194	63.02	15.93	0.26	15.91	125.75	0.01	125.86	Fructose
54.13	1.85	104578069	0.2082	62.00	31.92	10.61	9.64	51.30	1.83	24.01	Myo-inositol
39.18	2.00	50811411	0.1028	48.03	15.51	0.75	26.98	22.50	0.23	39.59	Gluconic acid
23.83	2.00	111712183	0.3697	40.27	0.37	0.09	61.15	0.26	18.68	121.58	glycerol
31.17	2.24	31424473	0.1087	40.01	13.22	0.31	18.76	20.58	0.47	29.56	B-Amino isobutyric acid
32.30	2.51	90927142	0.1847	38.35	19.21	1.39	16.41	24.46	0.12	17.43	Malic acid
43.90	1.71	18552006	0.0416	38.12	19.17	0.13	49.30	11.41	0.72	18.98	Fucitol
33.48	2.33	79450453	0.1766	37.74	15.69	14.10	15.80	0.04	0.00	0.03	Aspartic acid 1
28.97	3.20	40281112	0.0922	34.64	8.90	19.19	14.85	3.29	0.78	3.20	Aspartic acid 2
35.13	1.95	41701415	0.0812	32.27	33.52	0.31	27.25	13.15	1.68	10.83	L-Threonine acid
24.65	1.78	13032712	0.0394	30.78	0.80	0.53	13.28	0.01	32.53	23.62	1,2,3-butanetriol
18.12	2.20	126620339	0.3233	29.85	2.52	20.74	4.71	8.67	0.01	11.37	3-Hydroxyisobutyric acid
13.84	1.85	448199254	2.0928	27.79	12.92	0.17	24.30	9.82	0.09	15.55	Lactic acid

Table 2. Identified metabolites exhibiting the largest degree of variation (FDR) between strains

Identification of unknowns and validation of tentative hits using CI and accurate mass information

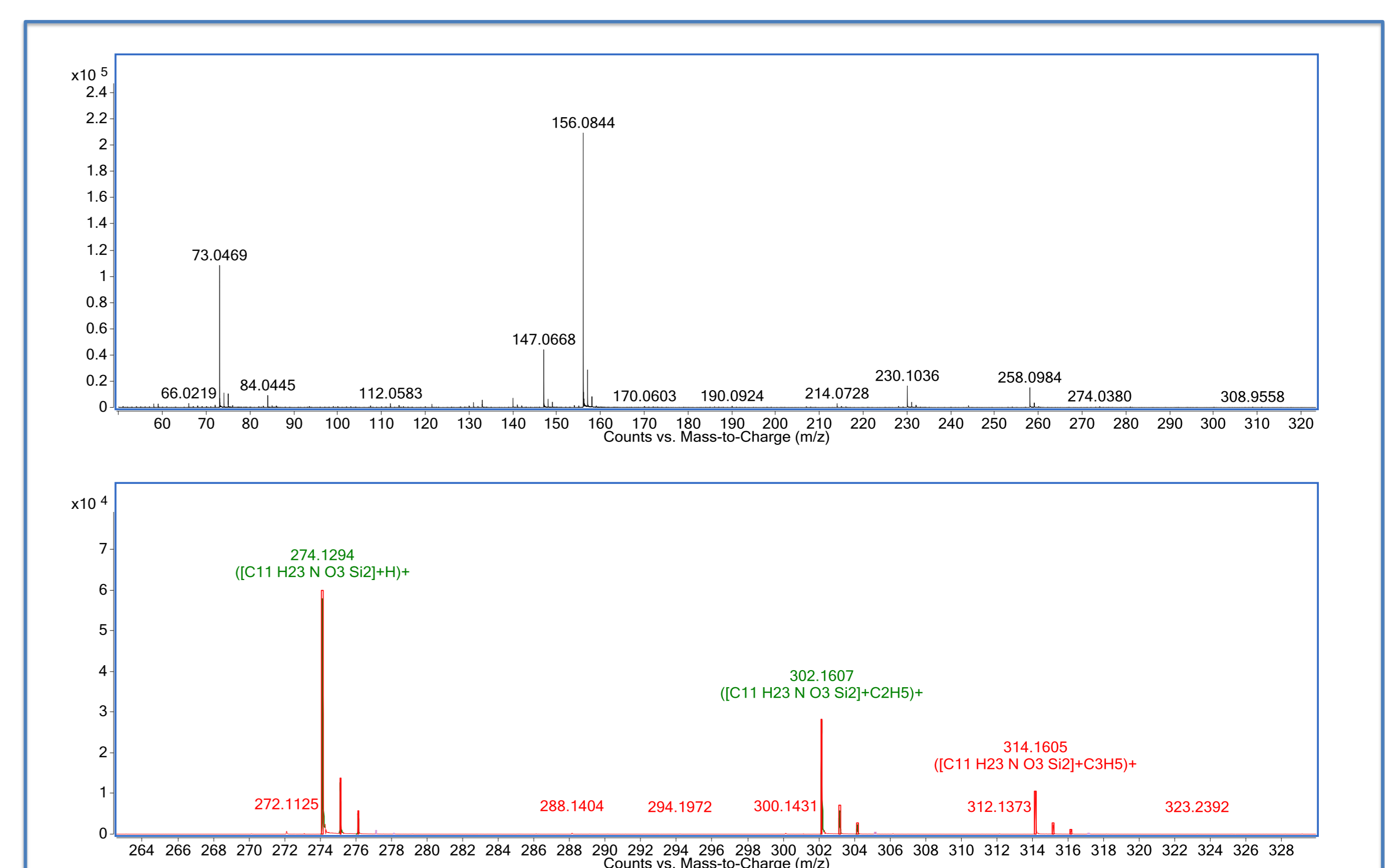


Fig 5. EI spectrum of tentatively identified pyroglutamic acid (upper) and its annotated MI cluster obtained with methane PCI (lower)

Conclusions

In this study, we employed GC x GC x QTOF methodology to compare partial metabolomes of a wild type isolate (Guy11) of *M. oryzae* to non-pathogenic mutant strains resulting from targeted deletion of key metabolic regulatory genes. Consistent with the role of the NUT1 gene in nitrogen metabolism, MDT1 in carbon metabolism, and TPS1 in integrating carbon and nitrogen metabolism, we observed significant changes in the carbon and nitrogen compounds identified in each strain compared to the wild type Guy11 isolate. These results provide evidence for how metabolic regulators ensure the correct assimilation of glucose and ammonium into metabolites important for infection. Notable changes include the requirement of functional Tps1 and Mdt1 proteins for the formation of glycerol, a metabolite important for turgor generation in the appressorium. Cystathionine metabolism is also shown to be misregulated in the mutant strains, and future work could be directed toward determining a role for metabolic pathways utilizing cystathionine during infection.